1 **Supplementary Information**

2

3 **Engineered bacterial outer membrane vesicles encapsulating oncolytic**

4 **adenoviruses enhance the efficacy of cancer virotherapy by augmenting tumor**

5 **cell autophagy**

6
7
8 **Ban et al.**

Supplementary Figures

Supplementary Figure 1. Qualitative analysis of P_2O expression in OMVs, *E. coli*@P_2O and

OMVs@P_2O. This experiment was repeated three times independently with similar results.
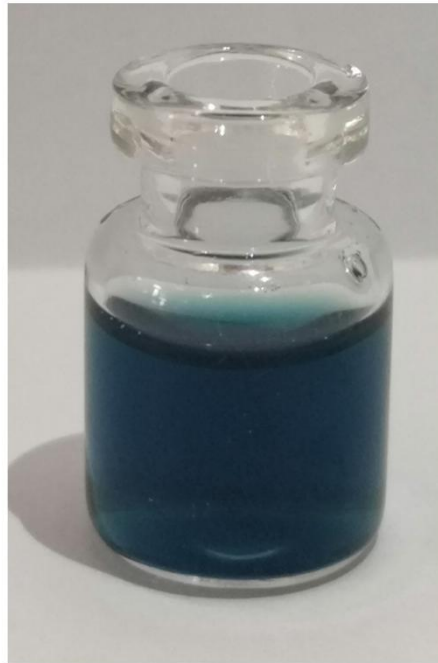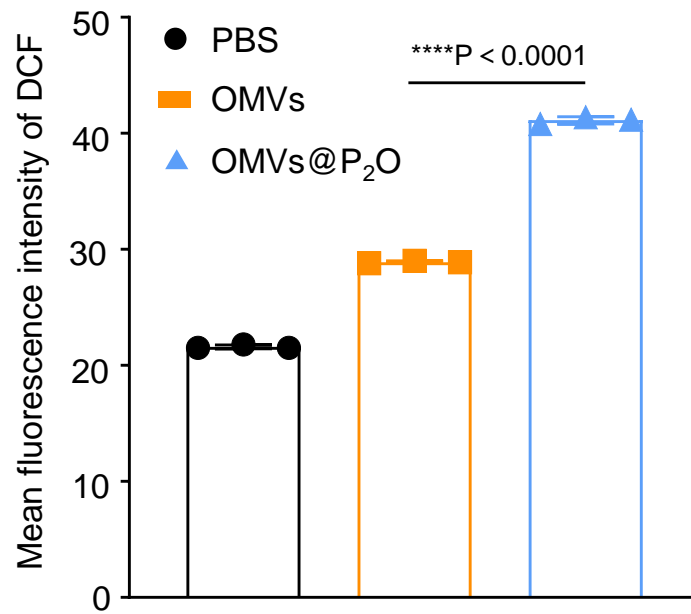
OMVs@P$_2$O-Ads

13

14 **Supplementary Figure 2.** Qualitative analysis of P$_2$O expression in OMVs@P$_2$O-Ads. This

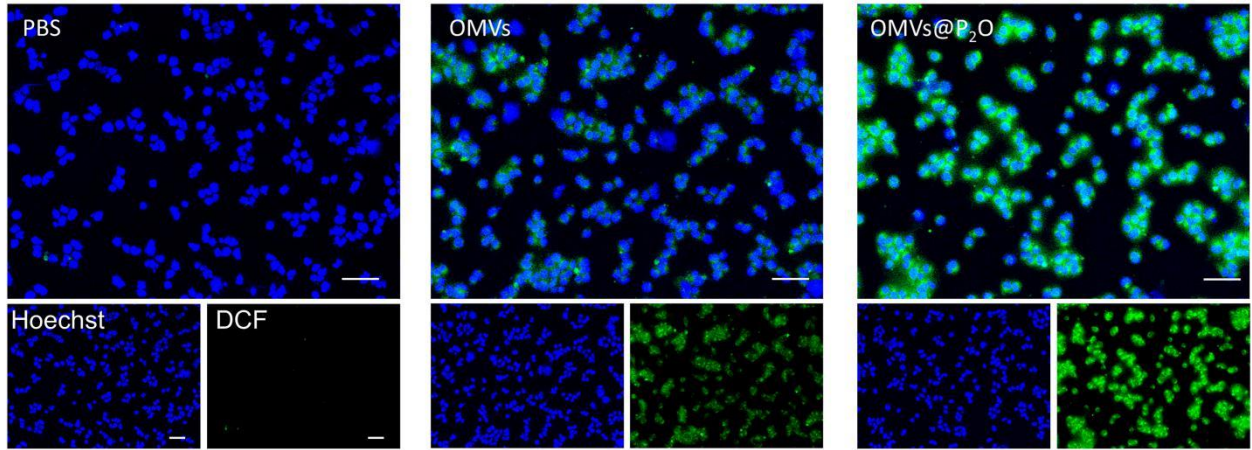15 experiment was repeated three times independently with similar results.

16

Supplementary Figure 3. Qualitative analysis of different concentration P_2O expression in OMVs@P_2O. This experiment was repeated three times independently with similar results.
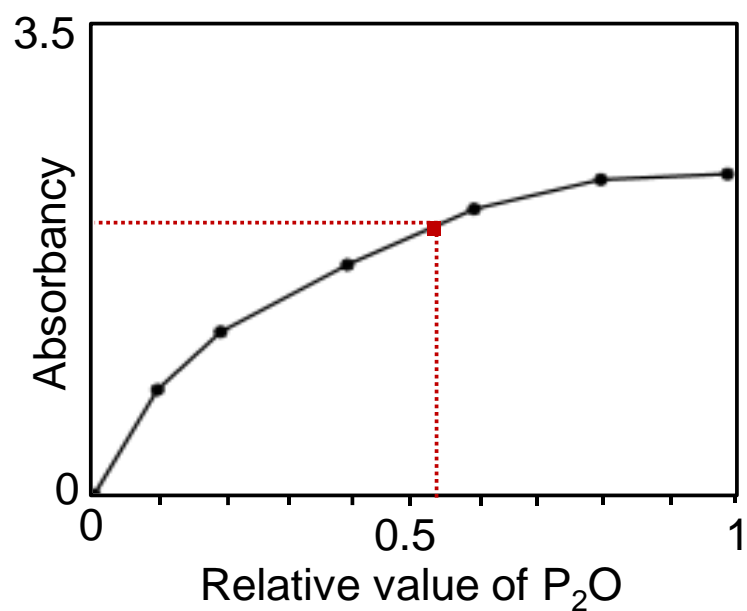
Supplementary Figure 4. The function curve illustrated the relationship between the absorbance and P_2O with different concentrations. The red point revealed the relative P_2O concentration within the microbial nanocomposite. Source data are provided as a Source Data file. This experiment was repeated three times independently with similar results.

24

Supplementary Figure 5. Quantitation of mean fluorescence intensity of DCF in PBS, OMVs and OMVs@P$_2$O for ROS level assessment in cells. Data are presented as mean ± SD (n = 3 independent experiments). ****P < 0.0001 by two-tailed Student's t-test. Source data are provided as a Source Data file.

29

Supplementary Figure 6. Immunofluorescence images of ROS expression in tumor cells in vitro. The cells were stained with DAPI (blue), and ROS were stained with DCF (green). Scale bars=100 μm. This experiment was repeated three times independently with similar results.

33
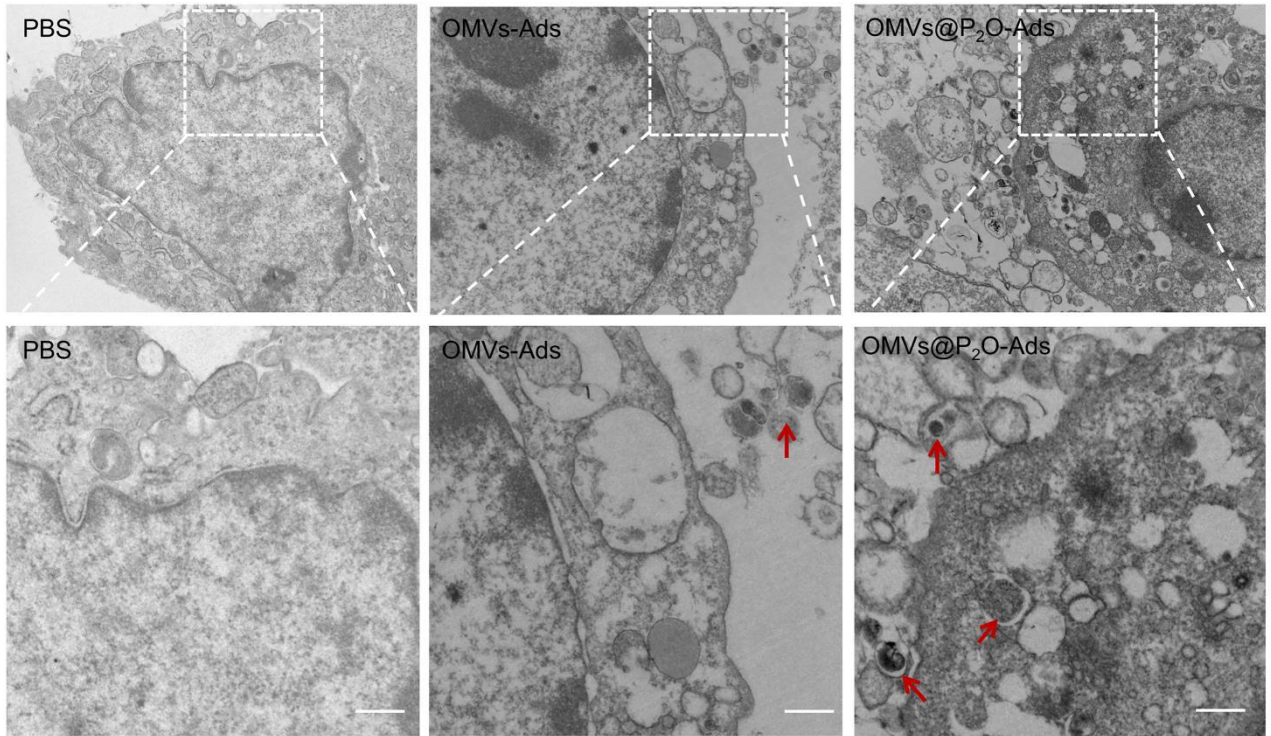
Supplementary Figure 7. The equal-scaling amplifying TEM images of autophagosomes, scale

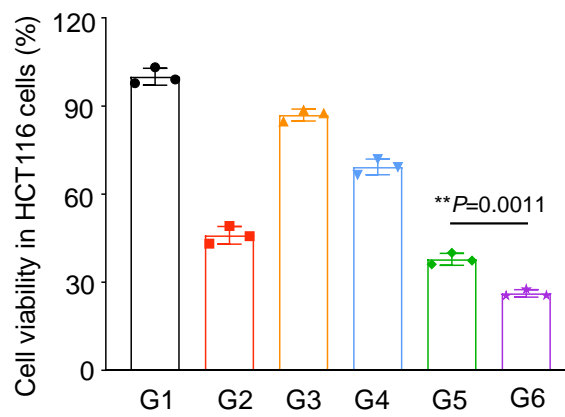bar=500 nm. This experiment was repeated three times independently with similar results.

36
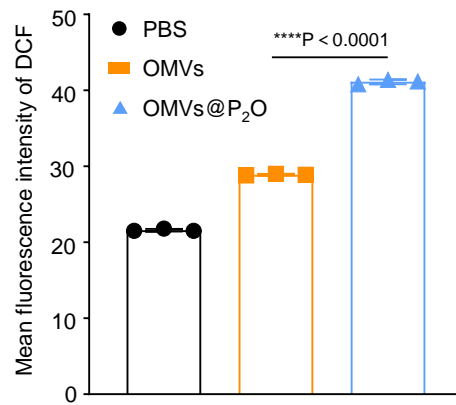
Supplementary Figure 8. The LC3-II/LC3-I ratio in vitro. Data are presented as mean ± SD (n = 3

independent experiments). **$P < 0.01$ by two-tailed Student's t-test. Source data are provided as a
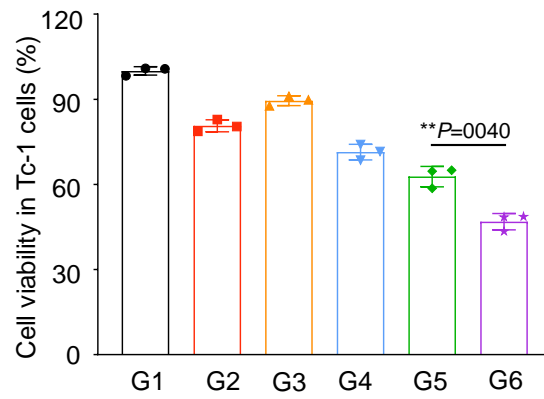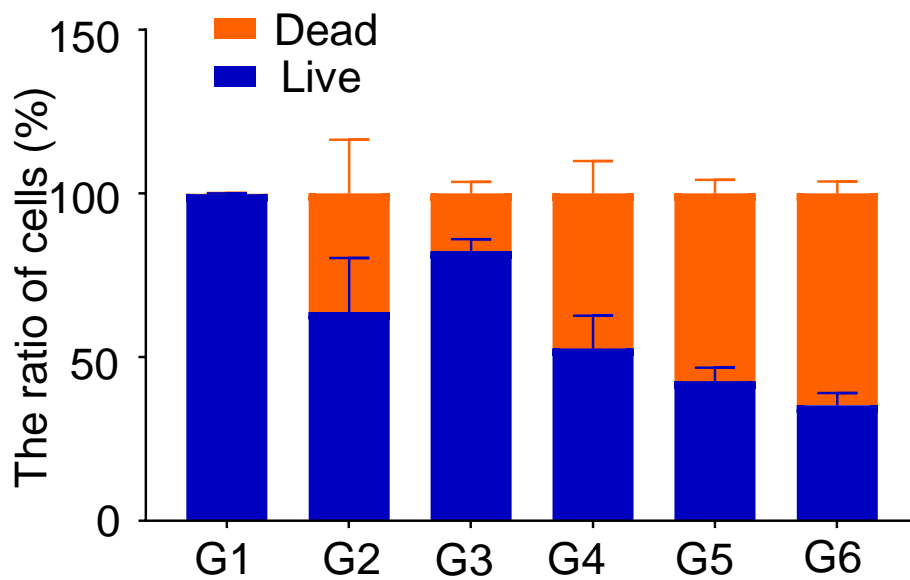
Source Data file.

40

41

42

43 **Supplementary Figure 9.** Cytotoxicity of different formulations in TC-1 cells and HCT116 cells

44 by MTT assay. Data are presented as mean $\pm$ SD (n = 3 independent experiments). **$P < 0.01$ by

45 two-tailed Student's t-test. Source data are provided as a Source Data file. (G1: PBS, G2: Ads, G3:
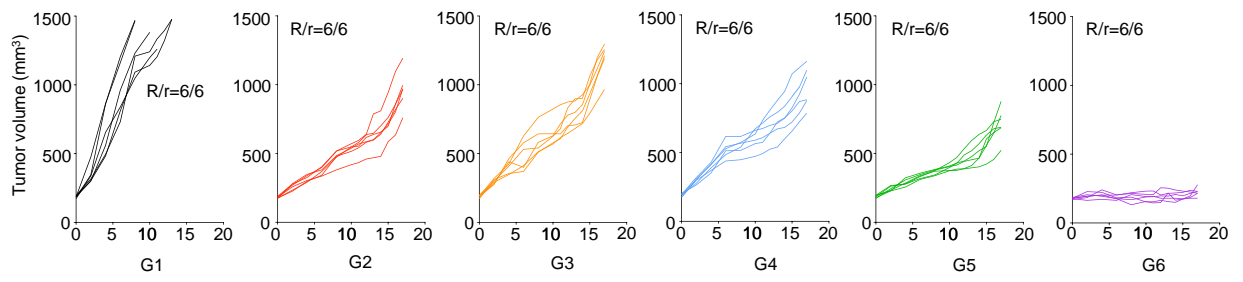
46 OMVs, G4: OMVs@P$_2$O, G5: OMVs-Ads, G6: OMVs@P$_2$O-Ads).

47

48

Supplementary Figure 10. The statistical analysis result of live/dead cellular staining. Data are presented as mean ± SD. Source data are provided as a Source Data file. (G1: PBS, G2: Ads, G3: OMVs, G4: OMVs@P$_2$O, G5: OMVs-Ads, G6: OMVs@P$_2$O-Ads). This experiment was repeated three times independently with similar results.

53

54
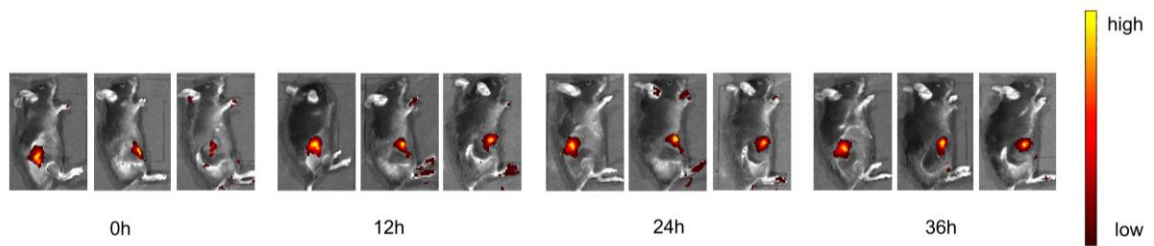
Supplementary Figure 11. In vivo DIR fluorescent imaging of the nanocomposite in TC-1-hCD46 xenograft tumor-bearing mice by IVIS (n = 4 mice).

57

Supplementary Figure 12. Individual tumor growth kinetics in different groups. (n = 6 mice).
Source data are provided as a Source Data file. (G1: PBS, G2: Ads, G3: OMVs, G4: OMVs@P$_2$O,
G5: OMVs-Ads, G6: OMVs@P$_2$O-Ads).

61
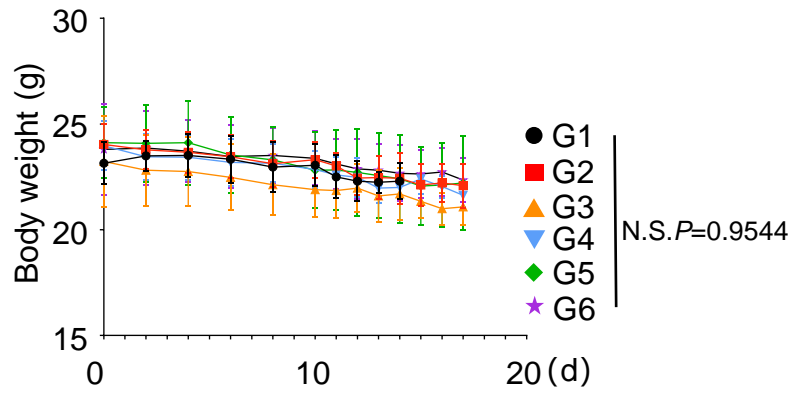
Supplementary Figure 13. Body weight changes of TC-1-bearing mice after intratumoral administration of different formulations. Data are presented as mean ± SD (n = 6 mice). N.S. (No Significance) $P > 0.05$ by two-tailed Student's t-test. Source data are provided as a Source Data file. (G1: PBS, G2: Ads, G3: OMVs, G4: OMVs@P_2O, G5: OMVs-Ads, G6: OMVs@P_2O-Ads).
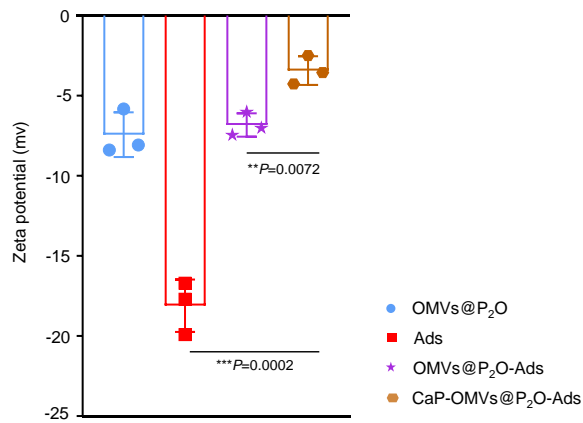
66
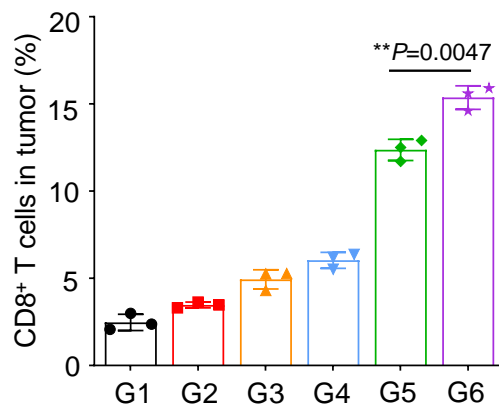
**Supplementary Figure 14.** The infiltration of CD8$^+$ T cells in tumor of mice treated with different agents on the 18th day. Data are presented as mean ± SD (n = 3 mice). **$P < 0.01$ by two-tailed Student's t-test. Source data are provided as a Source Data file. (G1: PBS, G2: Ads, G3: OMVs, G4: OMVs@P$_2$O, G5: OMVs-Ads, G6: OMVs@P$_2$O-Ads).

71

Supplementary Figure 15. Zeta-potential of OMVs@P_2O, Ads, OMVs@P_2O-Ads and CaP-OMVs@P_2O-Ads. Data are presented as mean ± SD (n = 3 independent experiments). **P < 0.01 and ***P < 0.001 by two-tailed Student's t-test. Source data are provided as a Source Data file.

75
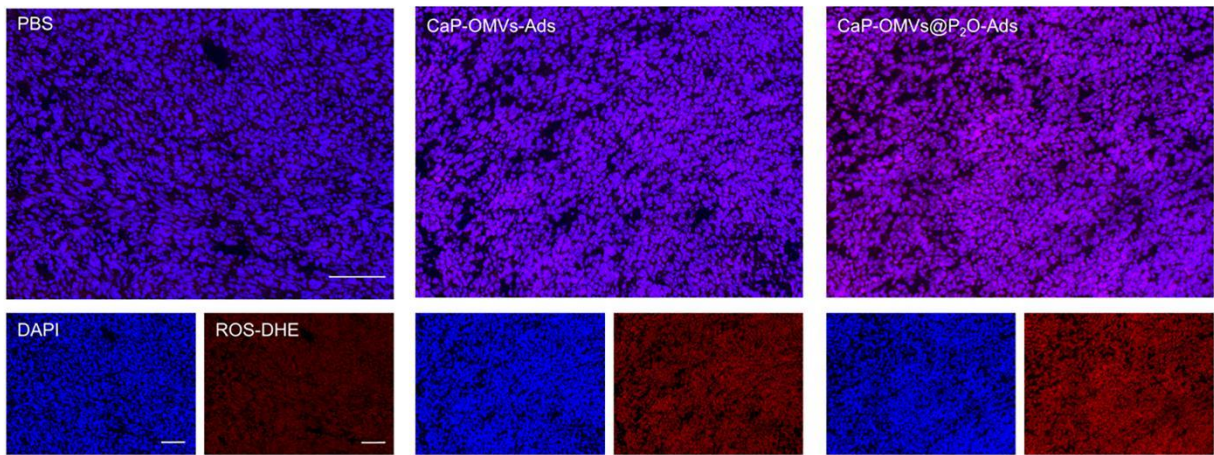
Supplementary Figure 16. Immunofluorescence images of ROS in tumor tissues. Blue represents DAPI-stained tumor cells and red represents DHE. Scale bar=100 μm. This experiment was repeated three mice with similar results.

79

80
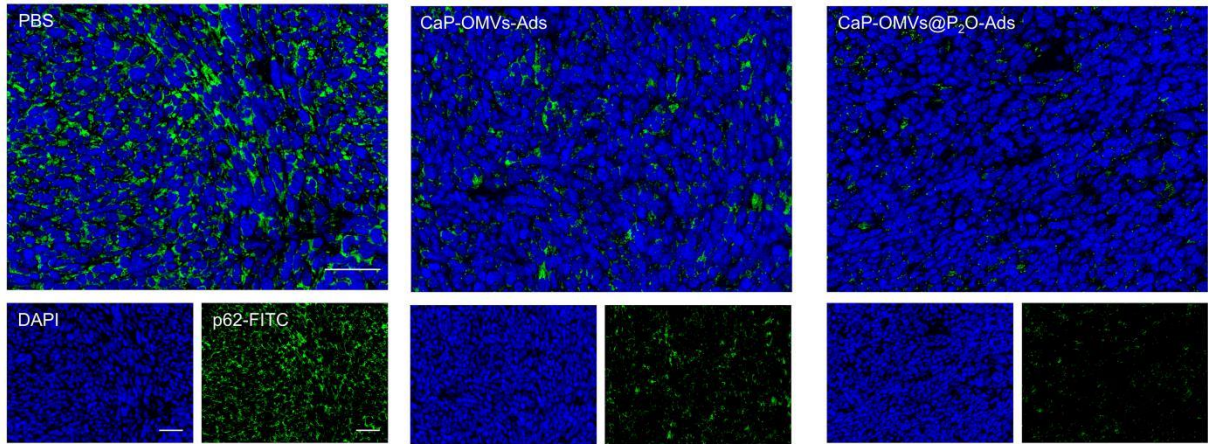
Supplementary Figure 17. Immunofluorescence images of p62 autophagic proteins in tumor tissues. Blue represents DAPI-stained tumor cells and the green represents FITC-stained p62 autophagic protein. Scale bar=50 μm. This experiment was repeated three mice with similar results.
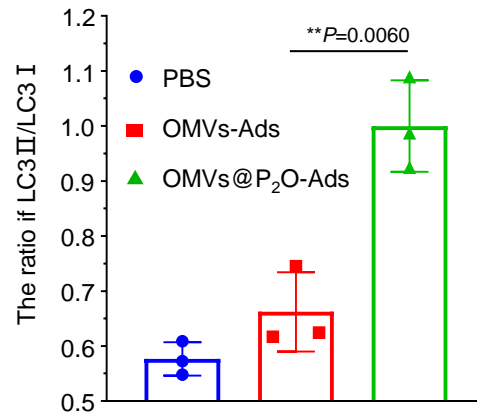
84

85   **Supplementary Figure 18.** The LC3-II/LC3-I ratio in vivo. Data are presented as mean ± SD (n =

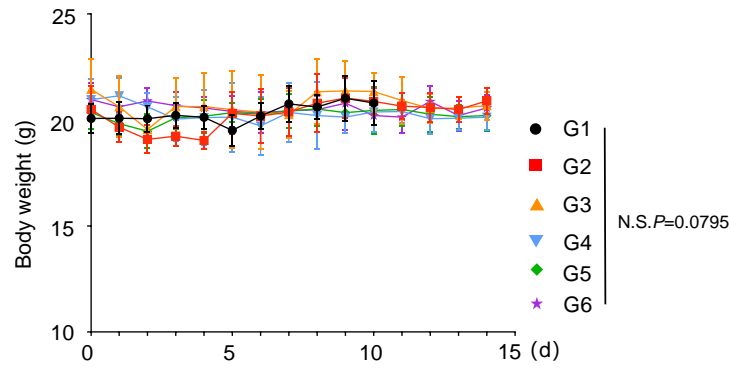86   3 mice). *$P < 0.01$ by two-tailed Student's t-test. Source data are provided as a Source Data file.

87
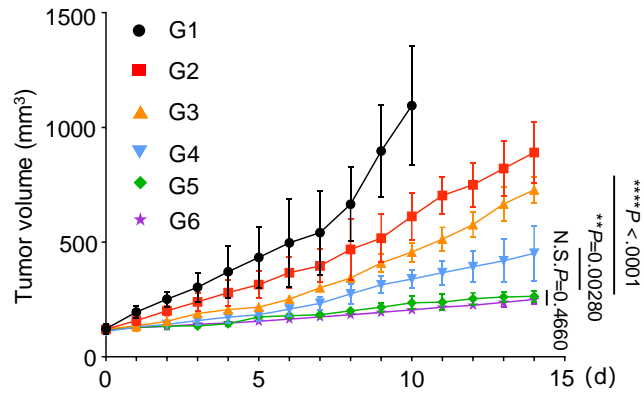
Supplementary Figure 19. The tumor of TC-1-bearing mice model volume change for TC-1 xenograft tumor model during different treatments. Data are presented as mean ± SD (n = 6 mice). N.S. (No Significance) $P > 0.05$, $**P < 0.01$ and $****P < 0.0001$ by two-tailed Student's t-test. Source data are provided as a Source Data file. (G1: PBS, G2: OMVs@P$_2$O-Ads, G3: CaP-OMVs-Ads, G4: Intra-Ads, G5: CaP-OMVs@P$_2$O-Ads, G6: Intra-Ads high does).

93

Supplementary Figure 20. Body weight changes of TC-1-bearing mice after administration of different formulations. Data are presented as mean ± SD (n = 6 mice). N.S. (No Significance) $P >$ 0.05 by two-tailed Student's t-test. Source data are provided as a Source Data file. (G1: PBS, G2: OMVs@P$_2$O-Ads, G3: CaP-OMVs-Ads, G4: Intra-Ads, G5: CaP-OMVs@P$_2$O-Ads, G6: Intra-Ads high does).
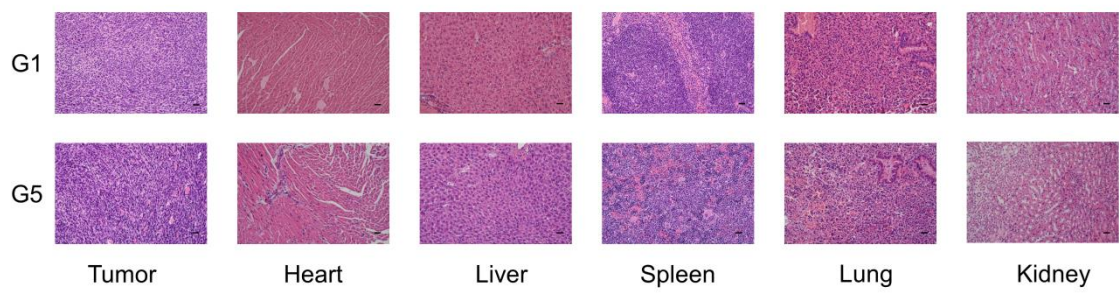
101

Supplementary Figure 21. Images of representative tumors after different treatments at 15 days (n=6). (G1: PBS, G2: OMVs@P$_2$O-Ads, G3: CaP-OMVs-Ads, G4: Intra-Ads, G5: CaP-OMVs@P$_2$O-Ads, G6: Intra-Ads high does).

105
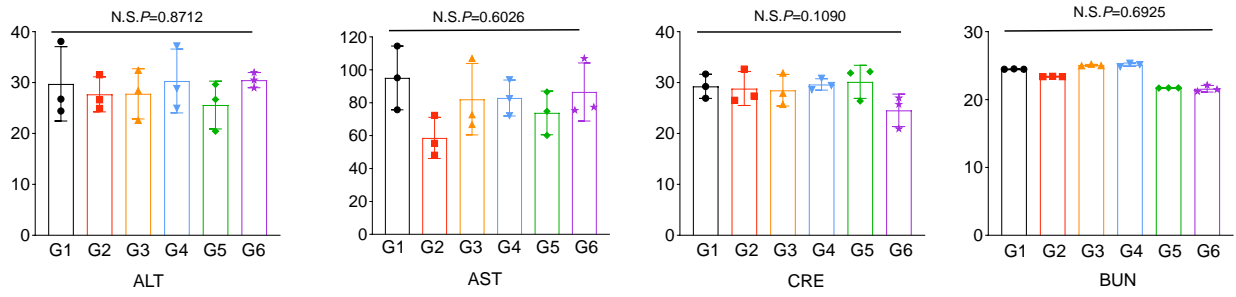
Supplementary Figure 22. Hepatorenal function indexes including aspartate aminotransferase (AST), alanine aminotransferase (ALT) levels, creatinine (CRE) and blood urea nitrogen (BUN) were measured. Data are presented as mean ± SD (n = 3 mice). N.S. (No Significance) $P > 0.05$ by two-tailed Student's t-test. Source data are provided as a Source Data file. (G1: PBS, G2: OMVs@P$_2$O-Ads, G3: CaP-OMVs-Ads, G4: Intra-Ads, G5: CaP-OMVs@P$_2$O-Ads, G6: Intra-Ads high does).

| | Tumor | Heart | Liver | Spleen | Lung | Kidney |

113

114   **Supplementary Figure 23.** H&E staining images for major organs slices after different treatments.

115   Scale bar=100 μm. This experiment was repeated three mice with similar results.
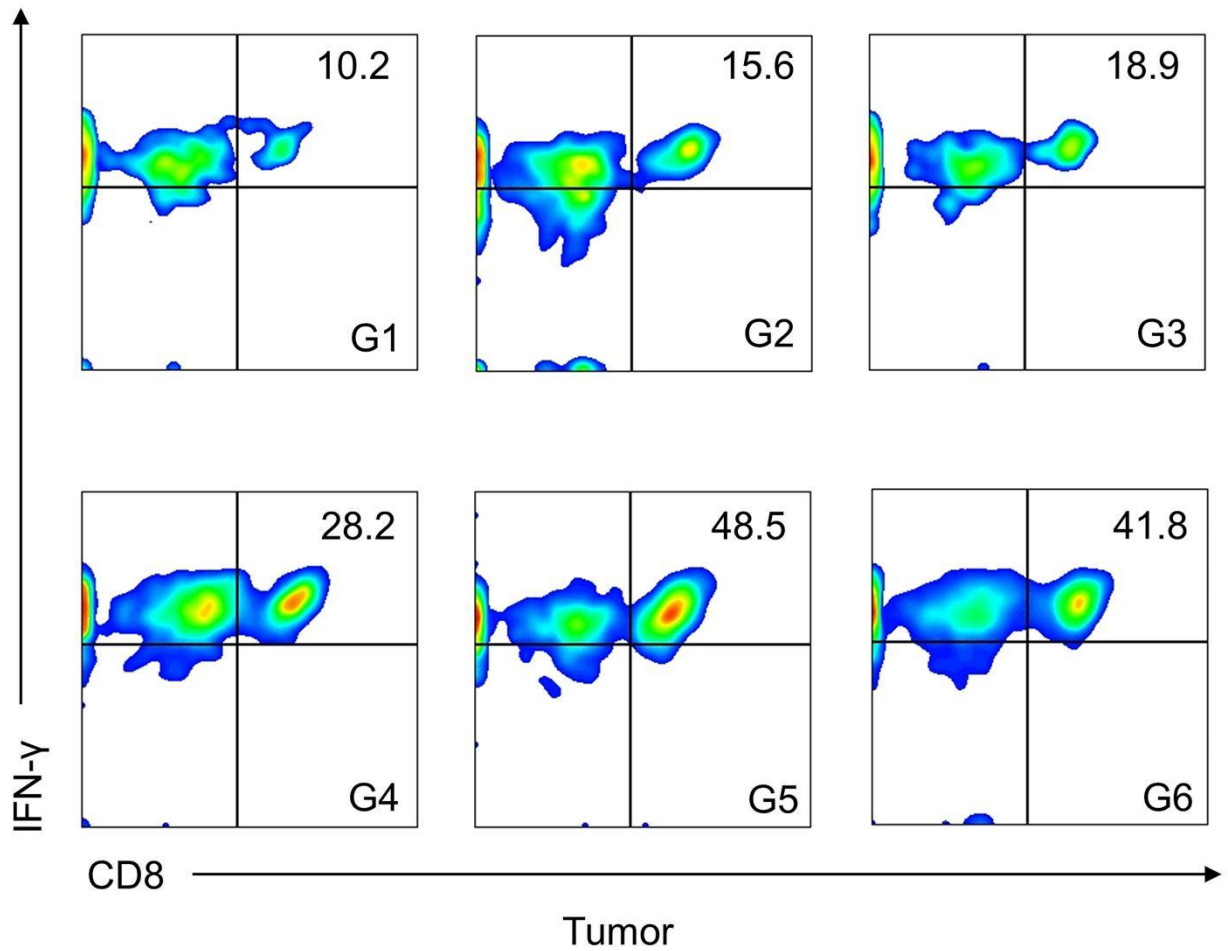
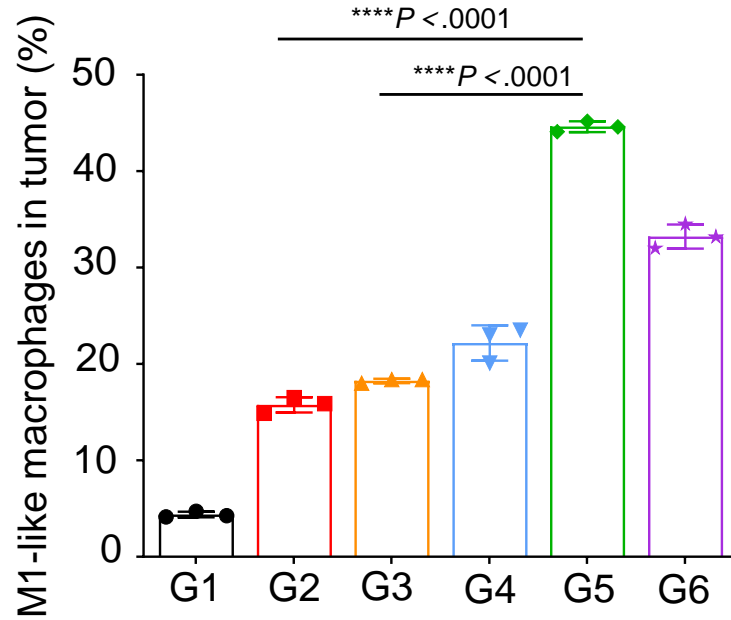**Supplementary Figure 24.** Representative flow cytometric evolution images of IFN-γ^+CD8$^+$ T cells (CD45$^+$CD3$^+$CD8$^+$IFN-γ^+) in tumor. (G1: PBS, G2: OMVs@P$_2$O-Ads, G3: CaP-OMVs-Ads, G4: Intra-Ads, G5: CaP-OMVs@P$_2$O-Ads, G6: Intra-Ads high does)
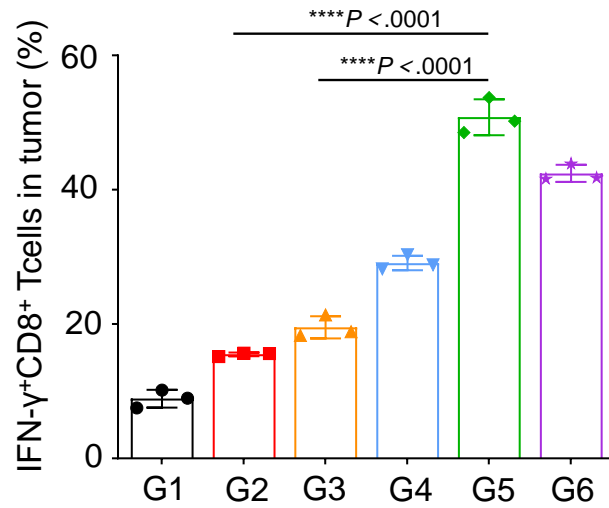
121

122 **Supplementary Figure 25.** Relative quantification of IFN-γ^+CD8$^+$ T cells
123 (CD45$^+$CD3$^+$CD8$^+$IFN-γ^+) in tumor. Data are presented as mean ± SD (n = 3 mice). ****$P <$
124 0.0001 by two-tailed Student's t-test. Source data are provided as a Source Data file. (G1: PBS, G2:
125 OMVs@P$_2$O-Ads, G3: CaP-OMVs-Ads, G4: Intra-Ads, G5: CaP-OMVs@P$_2$O-Ads, G6: Intra-Ads
126 high does)

127
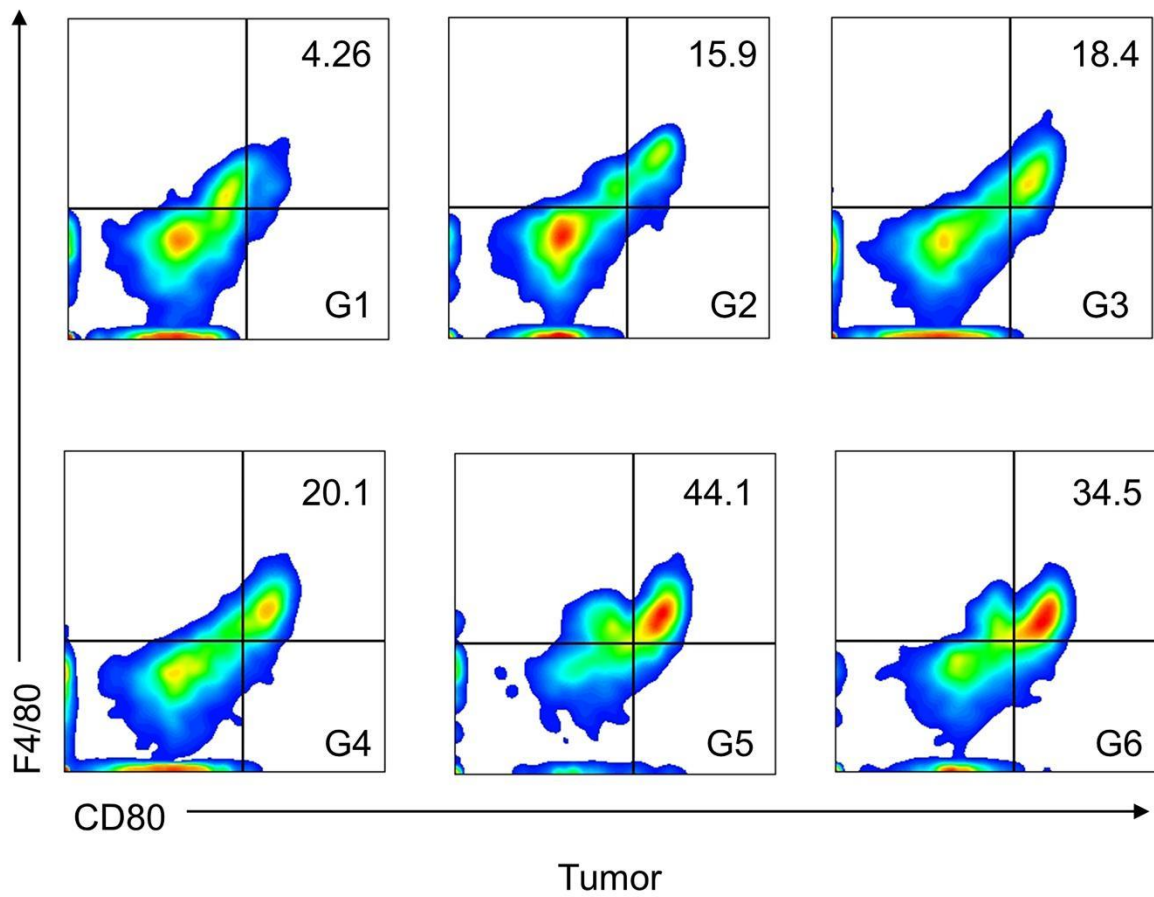
Supplementary Figure 26. Representative flow cytometric evolution images of M1-like macrophages ($CD45^+F4/80^+CD80^+$) in tumor (n=3). (G1: PBS, G2: OMVs@P_2O-Ads, G3: CaP-OMVs-Ads, G4: Intra-Ads, G5: CaP-OMVs@P_2O-Ads, G6: Intra-Ads high does)

131

Supplementary Figure 27. Relative quantification of M1-like macrophages (CD45$^+$F4/80$^+$CD80$^+$) in tumor. Data are presented as mean ± SD (n = 3 mice). ****P < 0.0001 by two-tailed Student's t-test. Source data are provided as a Source Data file. (G1: PBS, G2: OMVs@P$_2$O-Ads, G3: CaP-OMVs-Ads, G4: Intra-Ads, G5: CaP-OMVs@P$_2$O-Ads, G6: Intra-Ads high does)
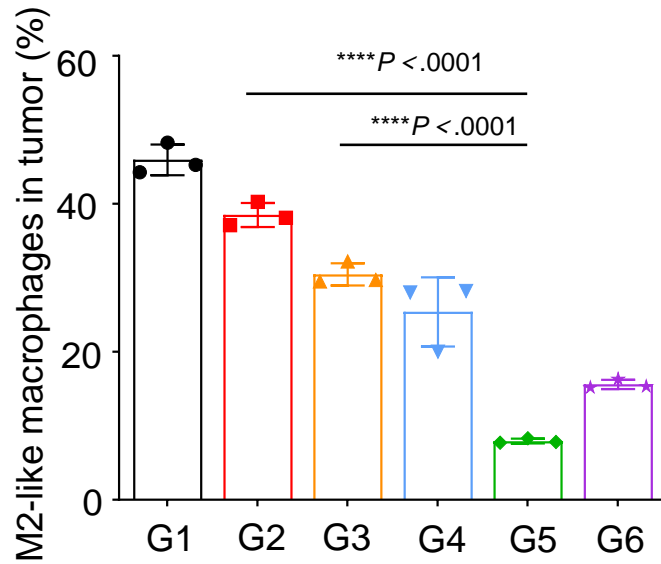
136
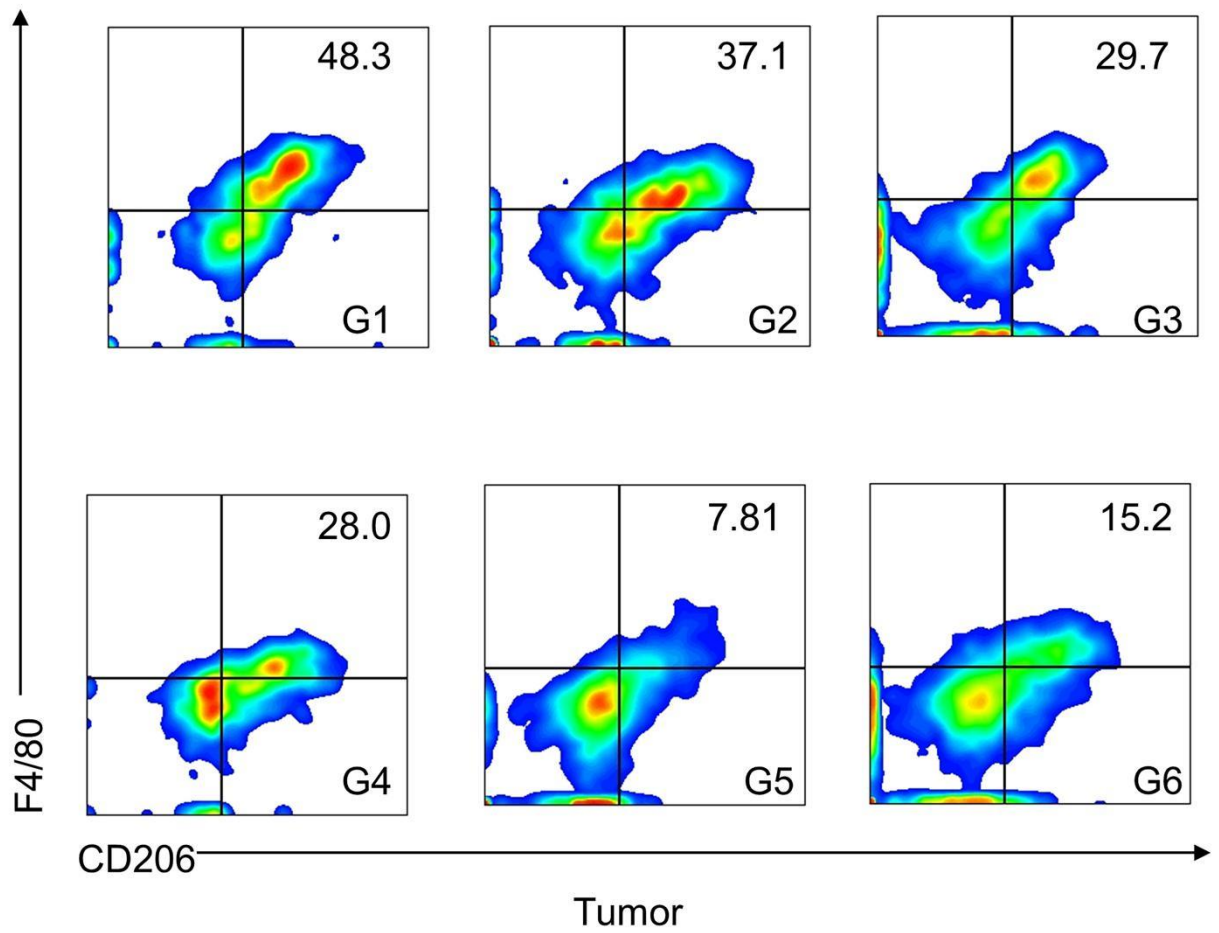
Supplementary Figure 28. Representative flow cytometric evolution images of M2-like macrophages ($CD45^+F4/80^+CD206^+$) in tumor (n=3). (G1: PBS, G2: OMVs@P_2O-Ads, G3: CaP-OMVs-Ads, G4: Intra-Ads, G5: CaP-OMVs@P_2O-Ads, G6: Intra-Ads high does)
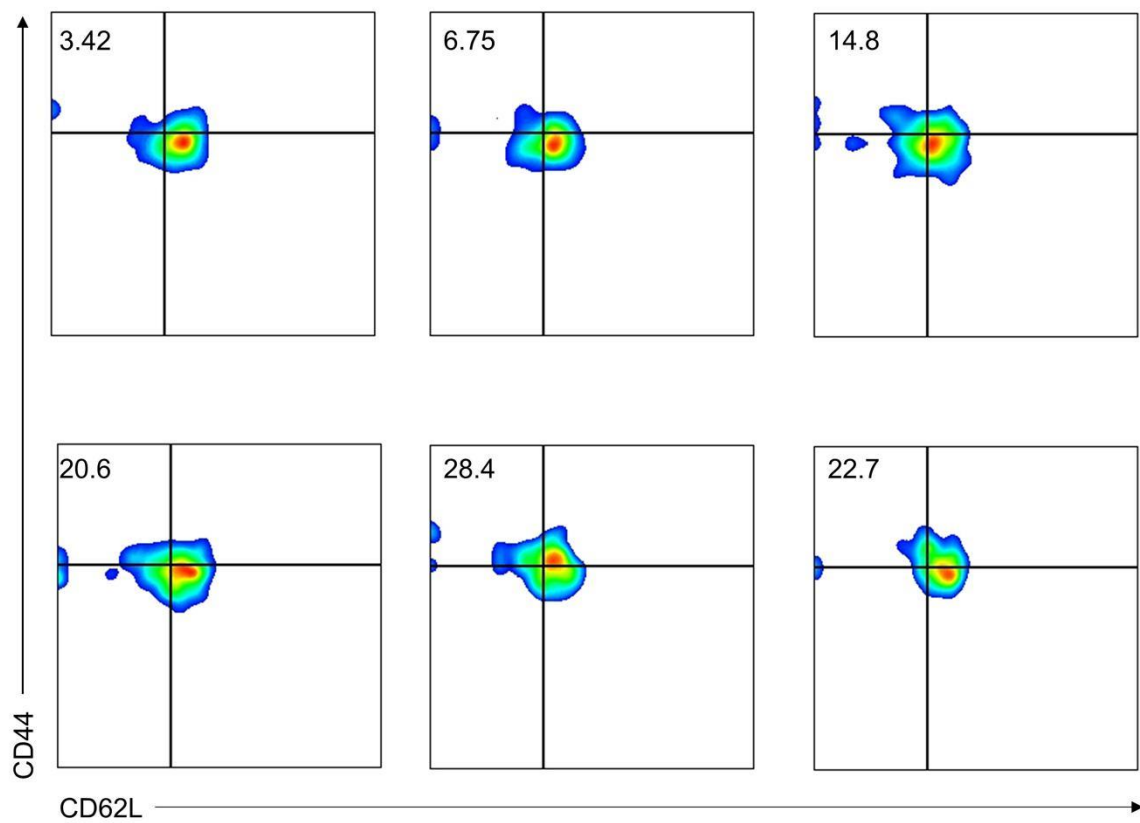
140

Supplementary Figure 29. Relative quantification of M2-like macrophages (CD45$^+$F4/80$^+$CD206$^+$) in tumor. Data are presented as mean ± SD (n = 3 mice). ****$P < 0.0001$ by two-tailed Student's t-test. Source data are provided as a Source Data file. (G1: PBS, G2: OMVs@P$_2$O-Ads, G3: CaP-OMVs-Ads, G4: Intra-Ads, G5: CaP-OMVs@P$_2$O-Ads, G6: Intra-Ads high does)
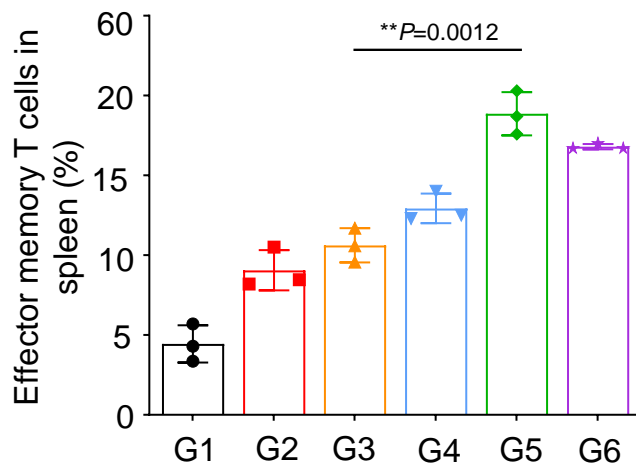
145

146

Supplementary Figure 30. The gating strategy of effector memory T cells (CD3$^+$ CD8$^+$ CD62L$^-$ CD44$^+$) in spleen. (G1: PBS, G2: OMVs@P$_2$O-Ads, G3: CaP-OMVs-Ads, G4: Intra-Ads, G5: CaP-OMVs@P$_2$O-Ads, G6: Intra-Ads high does).

150

Supplementary Figure 31. Relative quantification of effector memory T cells (CD3$^+$CD8$^+$CD62L$^-$CD44$^+$) in spleen. Data are presented as mean ± SD (n = 3 mice). **$P < 0.01$ by two-tailed Student's t-test. Source data are provided as a Source Data file. (G1: PBS, G2: OMVs@P$_2$O-Ads, G3: CaP-OMVs-Ads, G4: Intra-Ads, G5: CaP-OMVs@P$_2$O-Ads, G6: Intra-Ads high does)
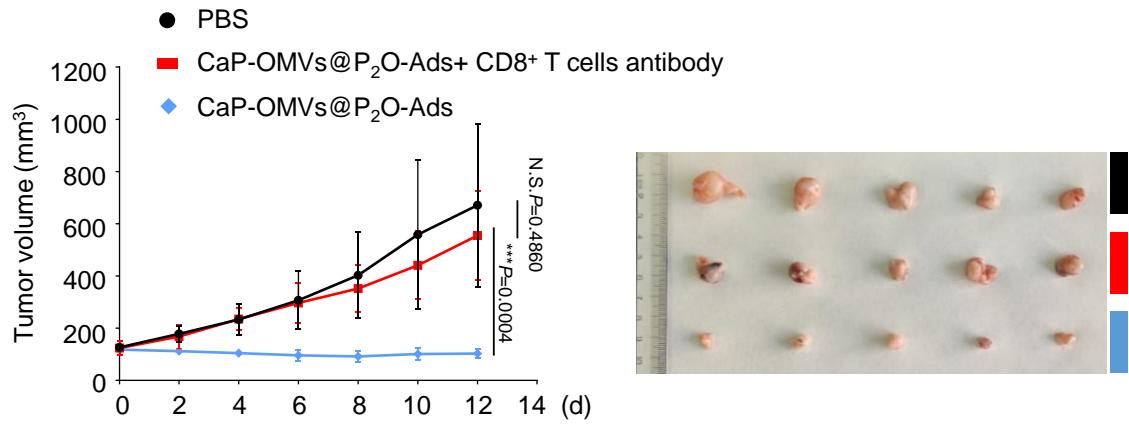
156
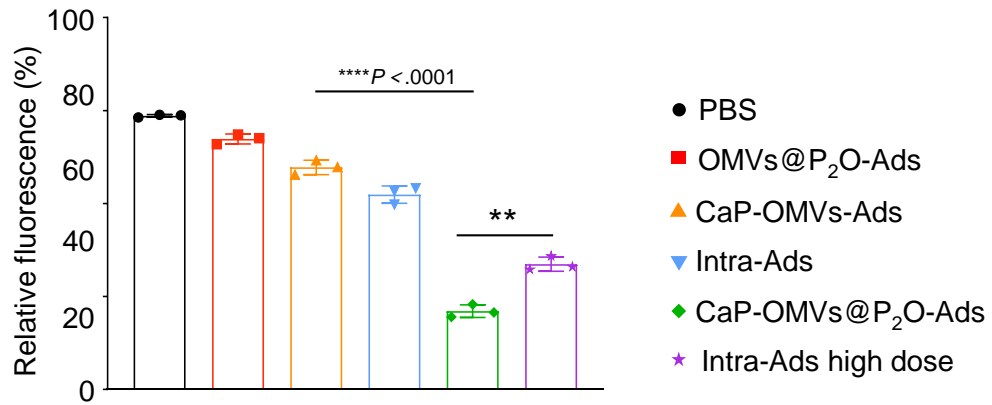
Supplementary Figure 32. The experimental result of the co-culture assay. Data are presented as mean ± SD (n = 3 independent experiments). **$P < 0.01$, ****$P < 0.0001$ by two-tailed Student's t-test. Source data are provided as a Source Data file. (It's worth noting here that PBS represents T cells extracted from mice in the PBS group, and other groups as above.)

Supplementary Figure 33. Images of representative tumors of different treated groups on the 12th day. Data are presented as mean ± SD (n = 5 mice). *P < 0.05, ***P < 0.001 by two-tailed Student's t-test. Source data are provided as a Source Data file.

165
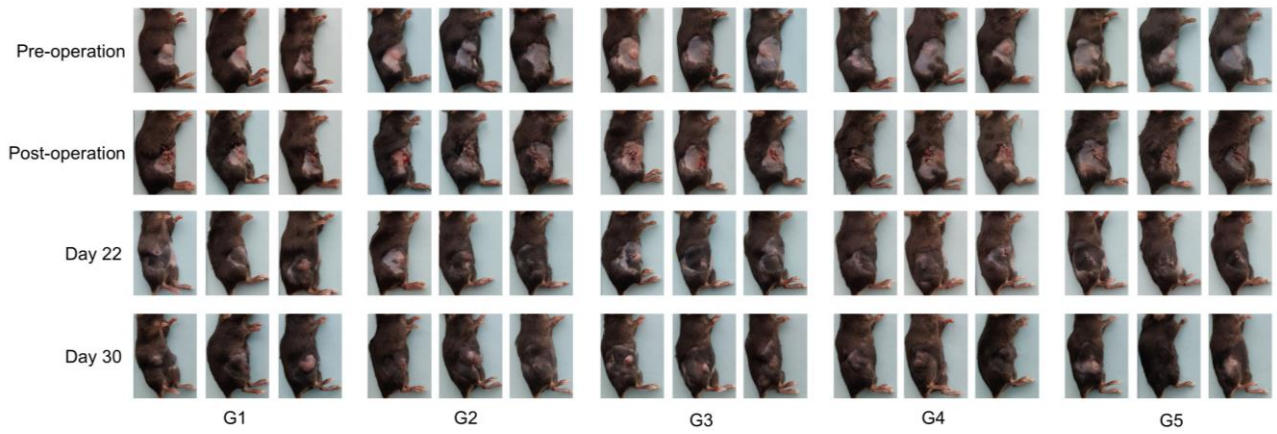
Supplementary Figure 34. Representative photos of primary tumor surgery and postoperative recurrence. (G1: PBS, G2: OMVs@P$_2$O-Ads, G3: CaP-OMVs-Ads, G4: Intra-Ads, G5: CaP-OMVs@P$_2$O-Ads).

169
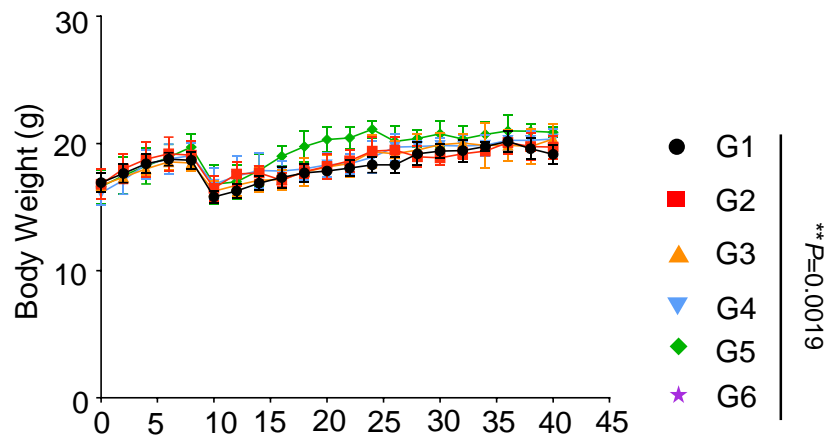
Supplementary Figure 35. Body weight changes of TC-1-bearing mice after administration of different formulations. Data are presented as mean ± SD (n = 5 mice). N.S. (No Significance) $P >$ 0.05 by two-tailed Student's t-test. Source data are provided as a Source Data file. (G1: PBS, G2: OMVs@P$_2$O-Ads, G3: CaP-OMVs-Ads, G4: Intra-Ads, G5: CaP-OMVs@P$_2$O-Ads).

174
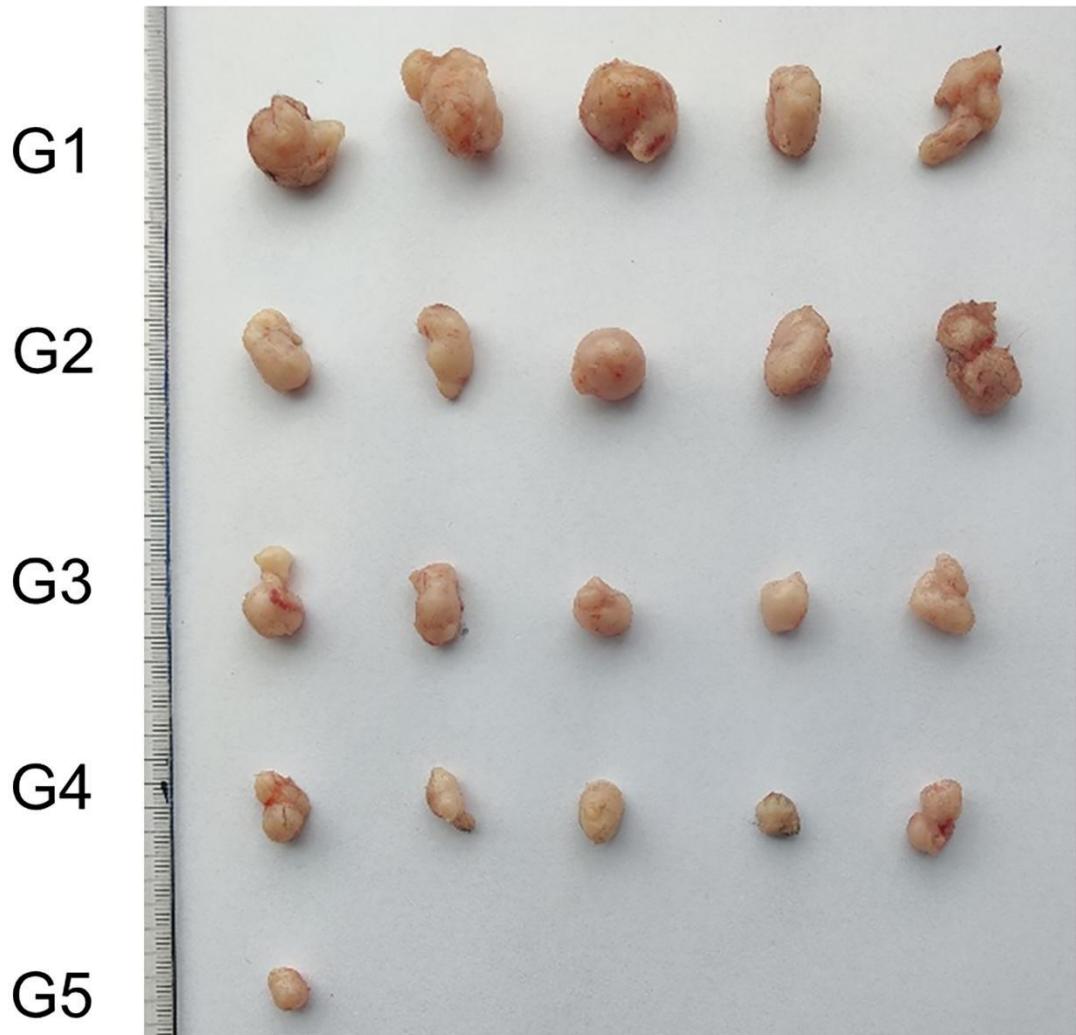
Supplementary Figure 36. Images of representative primary tumors after different treatments at 45 days (n=5). (G1: PBS, G2: OMVs@P$_2$O-Ads, G3: CaP-OMVs-Ads, G4: Intra-Ads, G5: CaP-OMVs@P$_2$O-Ads).

178

Supplementary Figure 37. Images of representative distant tumors after different treatments at 45 days (n=5). (G1: PBS, G2: OMVs@P$_2$O-Ads, G3: CaP-OMVs-Ads, G4: Intra-Ads, G5: CaP-OMVs@P$_2$O-Ads).

182
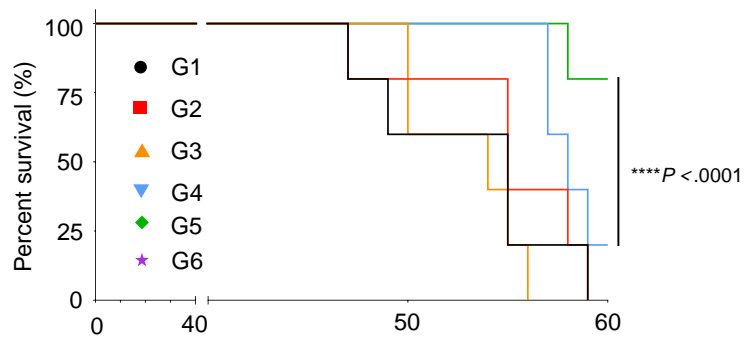
Supplementary Figure 38. Survival curves for treated bodies. Data are presented as mean ± SD (n = 5 mice). ****P < 0.001 by two-tailed Stude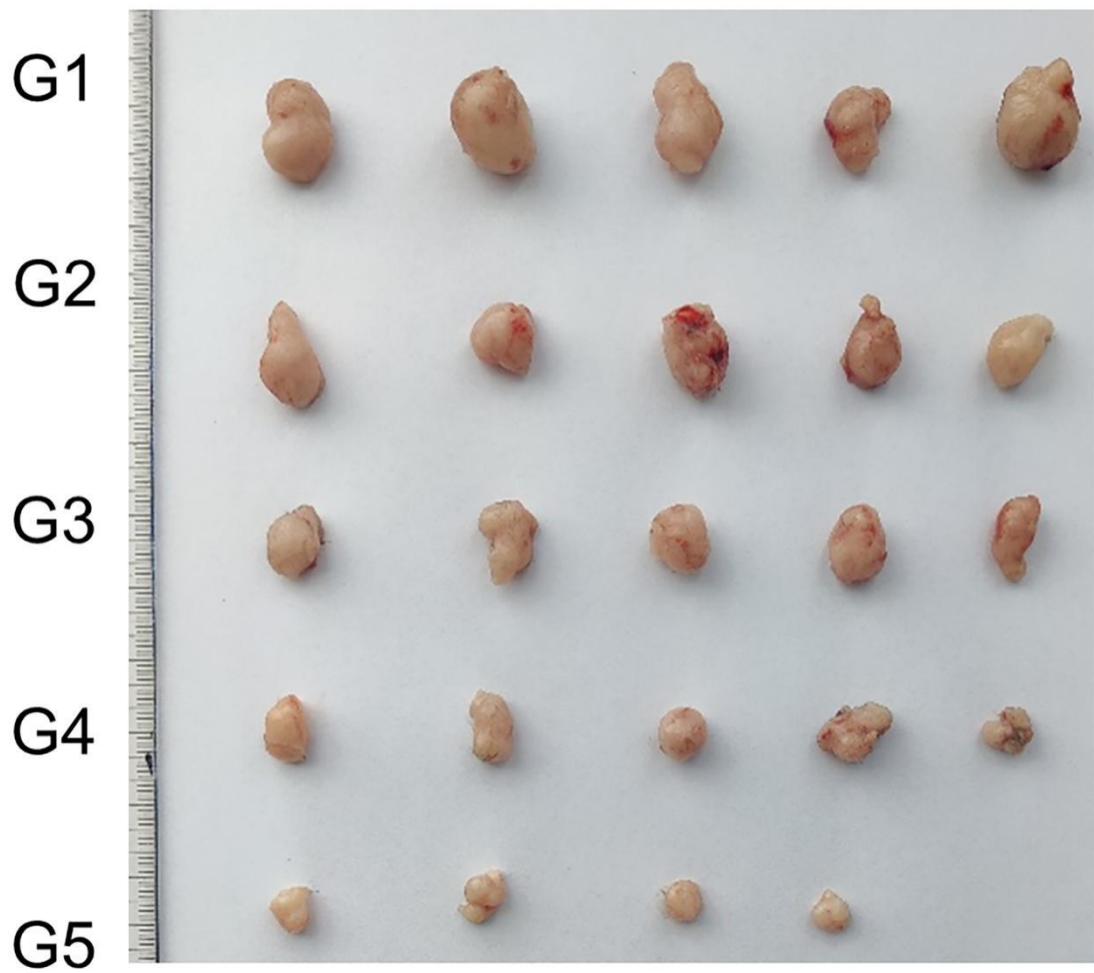nt's t-test. Source data are provided as a Source Data file. (G1: PBS, G2: OMVs@P$_2$O-Ads, G3: CaP-OMVs-Ads, G4: Intra-Ads, G5: CaP-OMVs@P$_2$O-Ad)
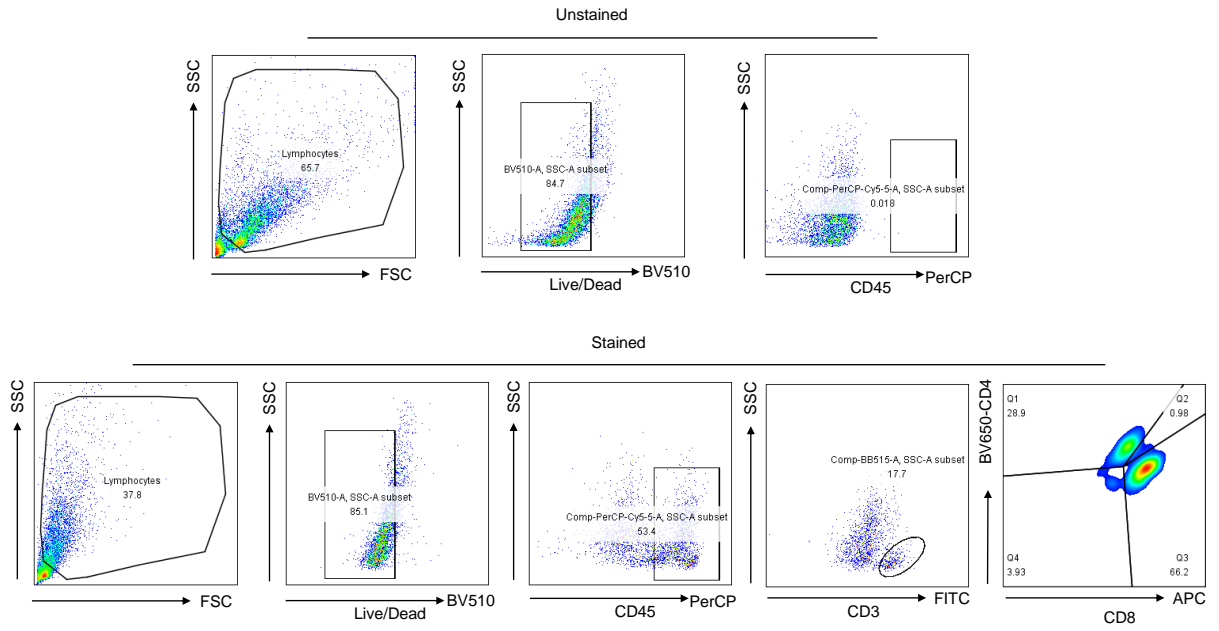
187

Supplementary Figure 39. The gating strategy of CD8$^+$ T cells (CD45$^+$CD3$^+$CD8$^+$) in the tumor.

(cf. Figure 5d and Supplementary Figures 14 and 24)

190
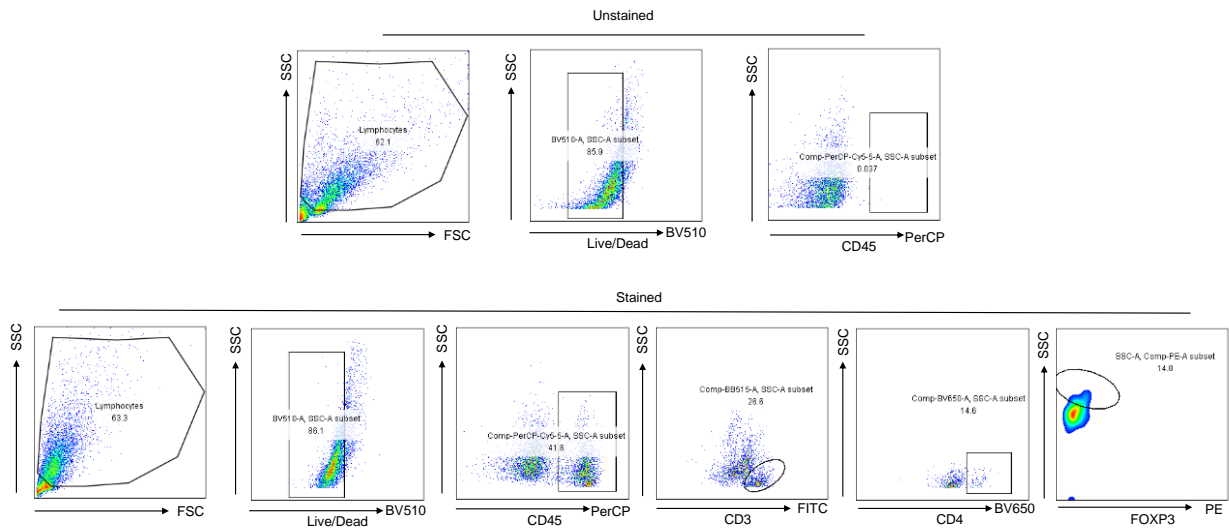
Supplementary Figure 40. The gating strategy of Treg cells (CD45$^+$CD3$^+$CD4$^+$FOXP3$^+$) in the tumor. (cf. Figure 5e)
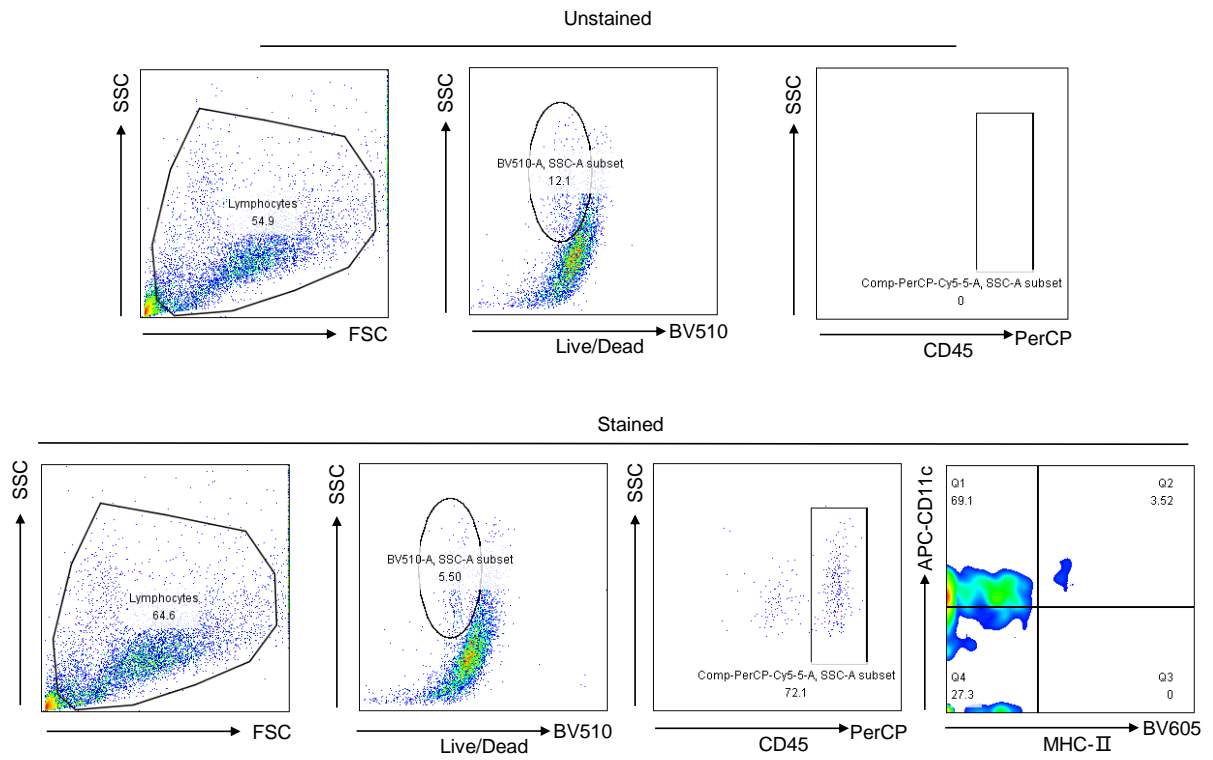
193

194 **Supplementary Figure 41.** The gating strategy of MHC-II$^+$ DC cells (CD45$^+$CD11c$^+$MHC-II$^+$) in

195 the tumor. (cf. Figure 5f)

196
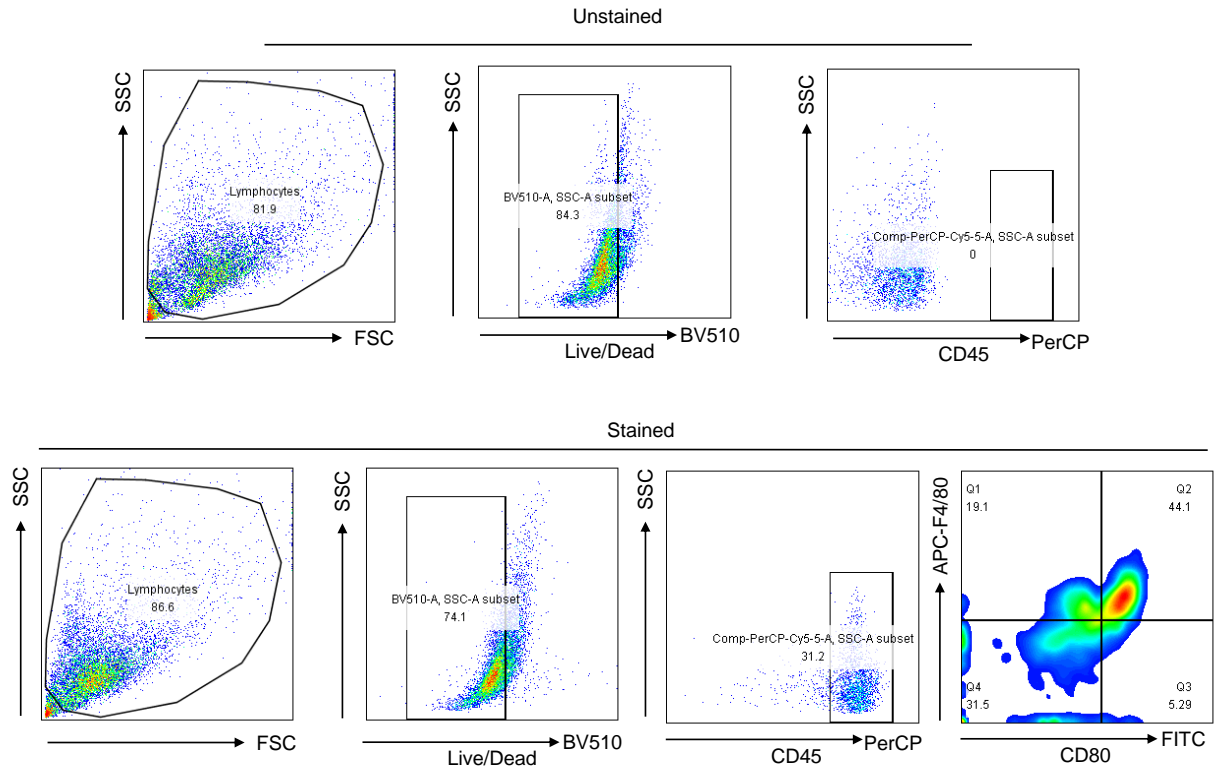
Supplementary Figure 42. The gating strategy of M1-like macrophages (CD45$^+$F4/80$^+$CD80$^+$) in tumor. (cf. Supplementary Figure 26)

199
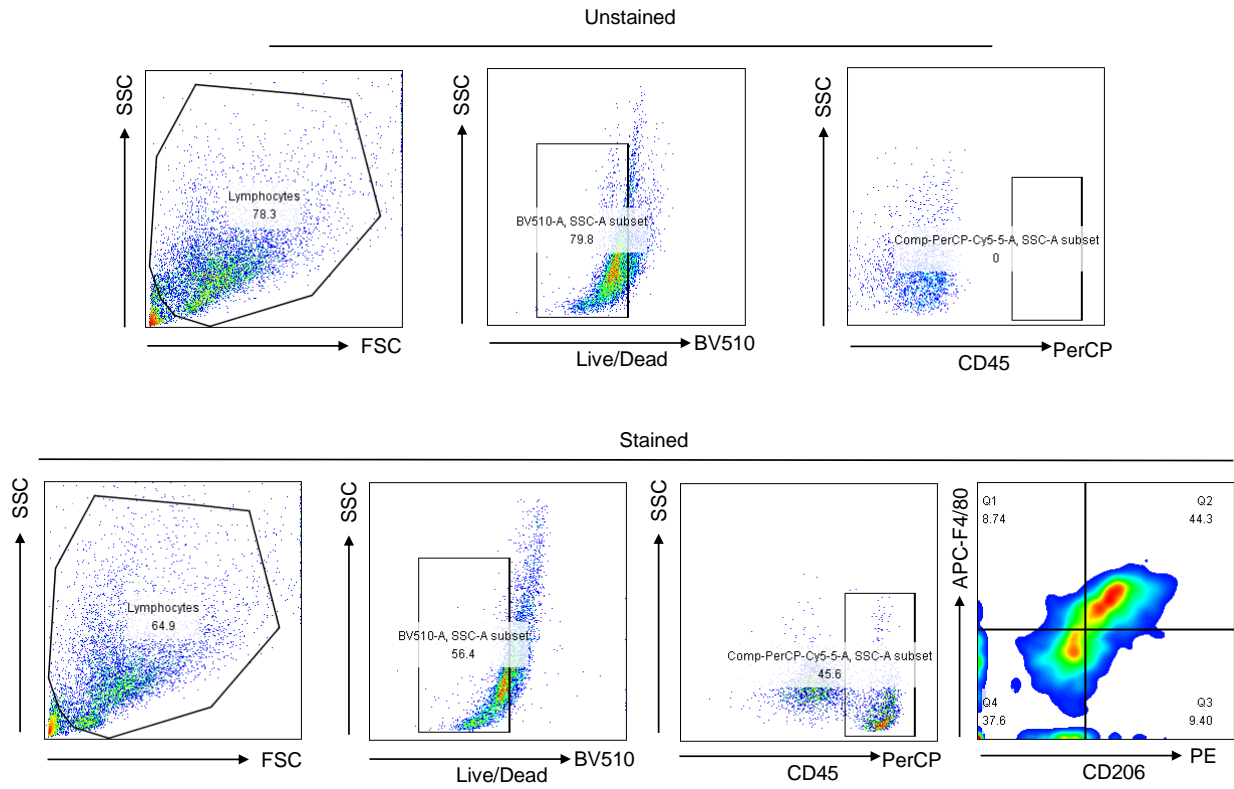
Supplementary Figure 43. The gating strategy of M2-like macrophages (CD45$^+$F4/80$^+$CD206$^+$) in tumor. (cf. Supplementary Figure 28)

202
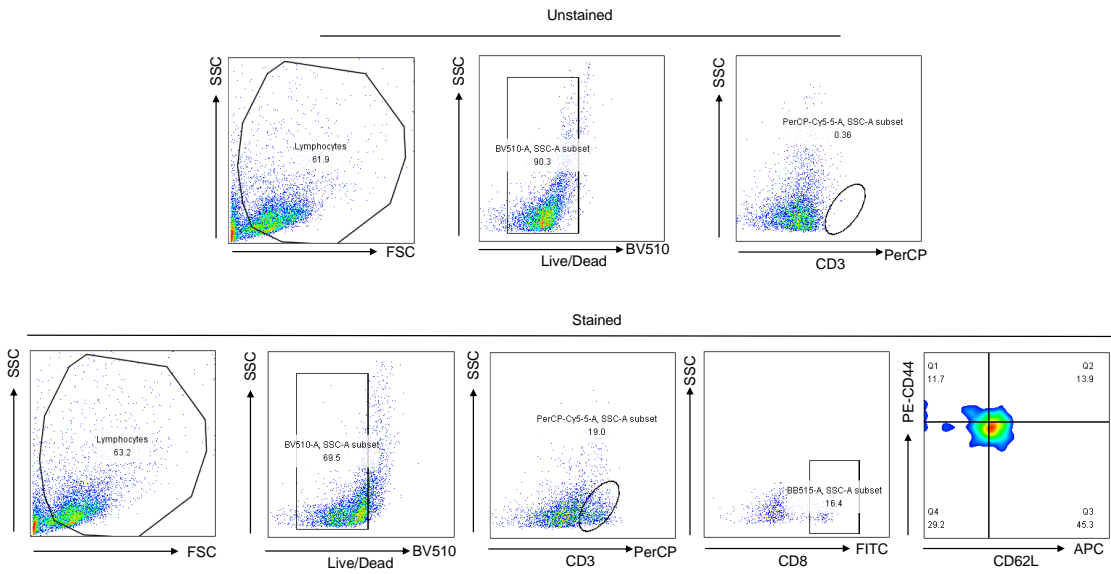
Supplementary Figure 44. The gating strategy of effector memory T cells (CD3$^+$ CD8$^+$ CD62L$^-$ CD44$^+$) in spleen. (cf. Supplementary Figure 30)

Supplementary Tables

Supplementary Table 1. Information on antibodies used in this study

Name	Dilution	Validation	Company name	catalog number	Clone number
LC3B pAb	1:1000	WB	ABCLONAL	A5601	No
SQSTM1/p62	1:100	IF	ABCLONAL	A11247	No
LC3B pAb	1:100	IF	ABCLONAL	A11282	No
CD8b Antibody	1:100	IF	Abmart Inc.	PK12778	No
CD45 Antibody	1:250	Flow	Biolegend	103130	30-F11
Fixable Viability Stain 510	1:250	Flow	BD Biosciences	564406	No
BV650 Rat Anti-Mouse IFN-γ(XMG1.2)	1:250	Flow	BD Biosciences	563854	XMG1.2
BV605 Rat Anti-Mouse I-A/I-E(M5/114.15.2)	1:250	Flow	BD Biosciences	563413	M5/114.15.2
CD3 Antibody	1:250	Flow	Biolegend	100204	17A2
CD8a Antibody	1:250	Flow	Biolegend	100712	53-6.7
FOXP3 Antibody	1:250	Flow	Biolegend	126404	MF-14
CD69 Antibody	1:250	Flow	BD Biosciences	562920	H1.2F3

MHC-II Antibody	1:250	Flow	BD Biosciences	563413	M5/114.15.2
CD11c Antibody	1:250	Flow	Biolegend	117324	N418
F4/80 Antibody	1:250	Flow	Biolegend	123118	BM8
CD62L Antibody	1:250	Flow	Biolegend	104428	MEL-14
CD44 Antibody	1:250	Flow	Biolegend	103008	IM7
CD80 Antibody	1:250	Flow	Biolegend	104714	16-10A1
CD206 Antibody	1:250	Flow	Biolegend	141706	C068C2
CD4 Antibody	1:250	Flow	BD Biosciences	563232	GK1.5
CD80 Antibody	1:250	Flow	Biolegend	104706	16-10A1
MOUSE CD8a	5mg	Injection	BIOXCELL	BP0061	No

207